

CFD Prediction of Supersonic Jet Impingement on Inclined Flat Plate

Antonio Mezzacapo(✉) and Giuliano De Stefano

Engineering Department, University of Campania Luigi Vanvitelli, 81031 Aversa, Italy
antonio.mezzacapo@unicampania.it

Abstract. This study aims at simulating the effects of turbulent supersonic jet impingement on an inclined flat plate, by examining the pressure distribution on the plate surface. Simulations are performed at the Mach number of 2.2, fixed the jet-to-plate distance, for different plate inclinations. Unlike previous studies, a modern turbulence modelling approach such as detached eddy simulation is followed, while comparing the current results to traditional unsteady Reynolds-averaged Navier-Stokes solution. It is determined that the DES solution is able to predict the correct pressure distribution on the plate, showing a quite good agreement against existing experimental and numerical data.

Keywords: Computational fluid dynamics · Turbulent supersonic jet · Unsteady Reynolds-averaged Navier-Stokes · Detached-eddy simulation

1 Introduction

Despite decades of research and progress, accurate and efficient computational fluid dynamics (CFD) simulation of wall-bounded supersonic turbulent flows still represents a challenging task, e.g. [1]. In particular, the research on free and impinging jets continues to receive a lot of attention by the applied CFD community, due to its high complexity. Indeed, the study of turbulent supersonic jets impinging on an inclined flat plate shows a strong interest in both theoretical research and engineering applications. The matter appears in various aerospace applications, including design of jet deflectors, and multistage rocket separation, among others [2].

The main advantage of CFD techniques is that they generally make less expensive to investigate a wider range of experimental parameters and configurations, compared to experimental methods. However, in spite of its geometric simplicity, the jet impingement on an inclined flat plate is very difficult to simulate, since the turbulent flow field involves a variety of complex fluid dynamics phenomena, including shock/shock and shock/boundary layer interactions. Due to the high computational cost, practically, the research resources have been mostly spent to investigate the impingement of perpendicular jets [3]. More recently, thanks to the surprising growth in computational power and the development of advanced numerical techniques, many research studies, as well as

© The Author(s), under exclusive license to Springer Nature Switzerland AG 2024
O. Gervasi et al. (Eds.): ICCSA 2024, LNCS 14814, pp. 366–377, 2024.
https://doi.org/10.1007/978-3-031-64608-9_24

comprehensive reviews [4], have focused on the flow field and the shock structures generated after the impact of impinging circular supersonic jet flows on various geometries and configurations. Specifically, varying nozzle to wall distance, nozzle diameter, and impingement angle have been considered [5].

As to experiments, the study carried out by Lamont and Hunt [6] represents one of the more significant works on supersonic jet impingement on inclined plates. Such study highlights how inclined jet impingement exhibits more complex features against the perpendicular case, due to strong shock-shock interactions. The latter can cause the maximum pressure on the inclined plate to be several times larger than that one attained for the perpendicular case, leading to more severe damage of the plate surface. The nozzle-plate distance, the jet pressure ratios, and the inclined angle of the plate all significantly impact on the jet flow characteristics. Other studies [7] highlighted how the flow structures generated at the impingement location are influenced by compressibility effects and fluid turbulence. In the research by Nakai et al. [8], the supersonic jet impinging on an inclined flat plate at various plate angles, pressure ratios, and nozzle-plate distances, was experimentally studied by using the pressure-sensitive paint (PSP) surface pressure measurement and the Schlieren method. From these experiments, Nakai and co-workers observed that there are three different types of flow patterns, and that, if the flat plate angle, nozzle-plate distance, and shock cell length are known ahead of time, it is possible to anticipate the different forms of flow. Furthermore, Ito et al. [9] carried out experiments of the jet impingement at higher flat plate angles, where the location and angle of the plate were changed from 1 to 4.5, and from 60 to 90°, respectively.

Most of the works available in the literature are mainly focused on the study of the acoustic field nearby the impingement zone. Although complex numerical techniques have been involved, such as large-eddy simulation, and hybrid Reynolds-averaged Navier-Stokes (RANS)/LES methods, little attention seems to have been given to the aerodynamic flow field. The objective of this ongoing research is to underline how the study of the acoustic field is not sufficient when examining a complex flow system such as jet impingement, where analyzing the aerodynamics field becomes a crucial point. The reason why many researchers in the past have focused their attention on the noise produced by the jet is associated to the so-called acoustic fatigue [10]. The intense acoustic pressures waves produced at the nozzle exit can actually cause failure of light weight structures, such as skin panels, fuselage rings and tail plane structures. While these failures may not be catastrophic, the associated maintenance and repair costs may be considerable. On the other hand, what the authors seem to have not been investigated enough is also the implication of the aerodynamic field on the impingement surfaces. For example, during the take off of an aircraft (or missile), the local increase of velocity produces a decrease of the local pressure near the impingement area, leading to a lose of lift. The latter may cause either takeoff failure or an excessive fuel consumption. Such phenomenon is known as lift loss, and was studied for the first time by Wyatt [11], using a baffle plate to simply represent the under surface of an aircraft. Conducting a series of experiments to

study the lift loss, due to a single air jet impinging on the ground at different heights, it found that closer was the ground surface from the jet, higher was the lift loss.

In this challenging context, the aim of this study is to determine and analyze the jet flow characteristics, and the pressure distribution on the flat plate, using modern CFD approaches. Unlike the similar previous study by Dharavath et al. [12], in which traditional unsteady RANS models were employed, a modern turbulence modeling approach that is detached-eddy simulation (DES) is investigated. The new results are compared with previous numerical and experimental data to demonstrate the capability of both approaches to predict and capture the correct pressure distribution over the plate and the complex flow structures created by the jet impingement, at several plate angles in the range between 30 to 50 °C.

2 CFD Model

2.1 Computational Domain

The flow geometry consists of an inclined flat plate and a convergent-divergent nozzle generating the supersonic jet. A schematic view of the computational domain is depicted in Fig. 1, with the flow region between the nozzle exit and the plate surface being represented in the zoomed-in picture. The domain extends up to $21D_j$, $75D_j$, $21D_j$, and $28D_j$, where D_j is the nozzle exit diameter, in the longitudinal direction, upper, lower, and lateral sections, respectively, in order to capture most of the complex flow field features. The rectangular flat plate has the dimensions of 50 m (length), 28 m (width), and 0.25 m (thickness). Note that the size of the present computational domain is reduced compared to reference simulations in [12]. Also, only the divergent section of the nozzle is simulated. Moreover, taking advantage of the expected symmetry of the resolved mean flow, only one half of the computational domain is actually considered in the practical simulations.

2.2 Computational Grid

Figure 2 shows an overview of the finite volume (FV) computational mesh, along with zoomed-in pictures corresponding to the flow region between the nozzle exit and the inclined plate. The method allows the complex compressible flow to be numerically approximated, with the conservation principles being applied over each control volume [13]. The FV mesh is made of a total of about 3 million cells, with structured elements in the close proximity of the plate (whose linear size is of the order of 0.05 m), and tetrahedral elements away from the plate. The meshing strategy allows on a smooth shift from structured to unstructured mesh elements, while reducing the computational complexity of the overall CFD model. In order to save computational time, the semi-empirical RNG $k - \epsilon$ turbulence model is employed, supplied with wall functions. The spatial discretization is performed

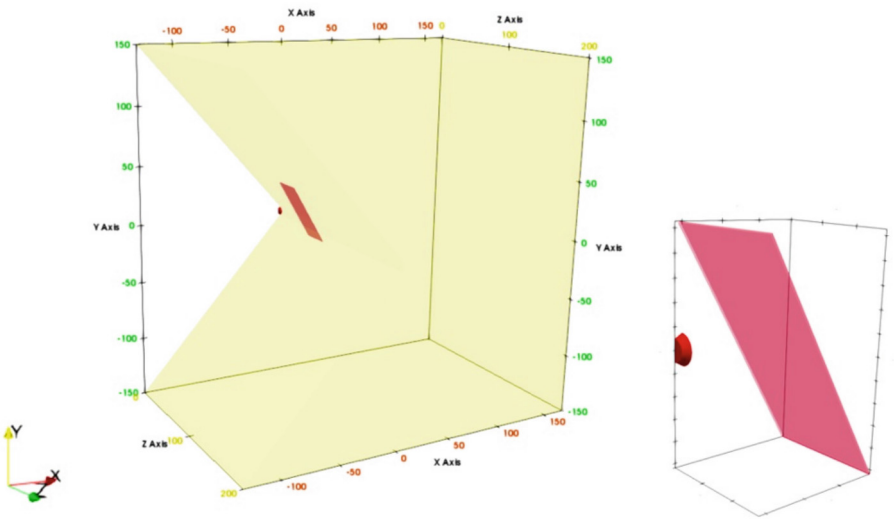

Fig. 1. Sketch of the computational domain, with zoomed-in picture of the flow region of primary interest.

by taking particular care to the height of the first computational cell, which is maintained at the order of 10^{-3} m, ensuring that $y^+ \approx 35$. The present wall modelled approach avoids to directly solve the entire boundary layer region, which would require a much more refined grid, resulting in saving approximately 4 million cells compared to the above mentioned reference work.

2.3 Boundary Conditions

Several numerical simulations are carried out using the commercial CFD software ANSYS Fluent [14], by considering different plate angles θ, fixed pressure ratio $PR = P_j/P_\infty$ (where P_j and P_∞ are nozzle exit and freestream pressures, respectively), and fixed distance between the nozzle exit and the plate surface L/D_j. The boundary conditions, which are based on the previous work by Dharavath et al. [12], are listed in Table 1. At the inlet, since the exact shape of the nozzle is given and known, a pressure-inlet boundary condition is imposed, where static pressure and temperature have been calculated under the assumption of isentropic flow. The pressure outlet condition is imposed at the outlet boundary. This allows to use the non-reflecting option, thus avoiding false reflections, but letting waves to pass through the boundaries.

Since the turbulent mean flow is expected to be symmetric, a symmetry boundary condition is imposed at $x = 0$, assuming a zero flux of all balanced quantities across the boundary. Finally, the no-slip boundary condition is used for the plate surface, where the fluid velocity is zero.

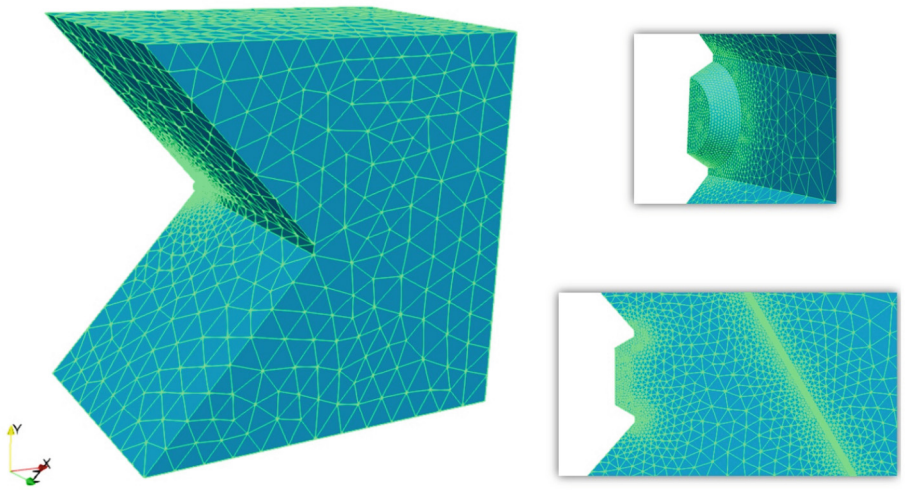

Fig. 2. Sketch of the computational grid, with zoomed-in pictures of the flow region of primary interest.

Table 1. Summary of boundary conditions

Boundary	Type
Inlet	Pressure inlet
Outlet	Pressure outlet
Plate	Wall
Symmetry	Symmetry plane

2.4 Numerical Parameters

For the different simulations that are conducted, the pressure ratio (P_j/P_∞) and the flat plate location (L/D_j) are kept constant, while varying the angle of inclination of the plate (θ). The characteristic compressible flow parameters are summarized in Table 2.

The double precision transient density-based solver is chosen for the following analysis due to its ability to handle highly compressible flows. Unlike the pressure-based solver, the pressure field is obtained from the equation of state while the density field is obtained using the continuity equation. Flow, energy and turbulence equations are accurately solved to obtain reasonable velocity and pressure gradients on the plate surface. The first order implicit Euler scheme is adopted for the time discretization, with the time step of $\Delta t = 10^{-4}$ s, making sure that the Courant number is kept approximately equal to 0.75 during all the time of the calculations. The threshold for the residual criterion for both momentum and energy is set equal to 10^{-6}, and the maximum iterative loop is made of 6 iterations for each time step. Finally, under-relaxation factors for turbulence kinetic energy (k) and turbulence dissipation rate (ϵ) are set to 0.75, in order to increase the stability of the iterative process.

Table 2. Characteristic flow parameters

Boundary	Values
Stagnation pressure, Pc	100 kPa
Stagnation temperature, Tc	298 K
Nozzle exit Mach number, M_j	2.2
Pressure ratio, $PR = P_j/P_\infty$	7
Specific heat ratio, γ	1.4
Plate angle, θ	30°, 40°, 50°
Nozzle exit diameter, D_j	7 m
Plate location, L/D_j	2

3 Results

Two different turbulence modeling approaches are employed in order to assess the predictive capabilities of the present CFD model to simulate the plume impingement flow field on the inclined flat plate. As preliminary step of the ongoing research, a variant of the standard semi-empirical $k-\epsilon$ turbulence model is investigated, namely, the RNG $k-\epsilon$ model [15]. This model is well known for its robustness, economy, and reasonable accuracy, for a wide range of industrial fluids engineering applications. It represents an improved version of the original $k-\epsilon$ model, resulting more accurate to simulate the spreading rate of both planar and round jets [16]. Although the original version of the model and its variations are known to be more suitable for free shear flow regions away from the wall, Dharavath et al. [12] demonstrated that different turbulence URANS methods (including the RNG $k-\epsilon$ model) provide similar surface pressure distributions for the present flow configuration with $\theta = 30°$. Here, the RNG $k-\epsilon$ turbulence model is confirmed to provide accurate mean flow results, in agreement with the reference study, where a different commercial code was employed [12].

The main point of the present CFD analysis involves the usage of a more innovative and sophisticated turbulence modeling procedure that is DES. In particular the realizable $k-\epsilon$ based DES model is employed. Figure 3 shows the pressure distribution on the plate for the two different solutions, namely URANS and DES, for varying plate incidence, compared to the experimental findings in [8]. In these plots, the distance Y is nondimensionalized by the nozzle exit radius R_n, whereas the pressure is nondimensionalized by the nozzle chamber pressure P_c. By inspection of this figure, both solutions appear to correctly reproduce the pressure peak and its location on the plate, when compared against experimental results, regardless of the plate incidence. In fact, a pretty good match of pressure distribution for the three different plate inclinations, which are θ= 30°, 40°, and 50°, against the experimental data, is attained. It is interesting to note that the location and pattern of impingement seems to change with the plate inclination, and it becomes more noticeable at high incidences, confirming previous findings. The same trend is observed for both URANS and DES approaches.

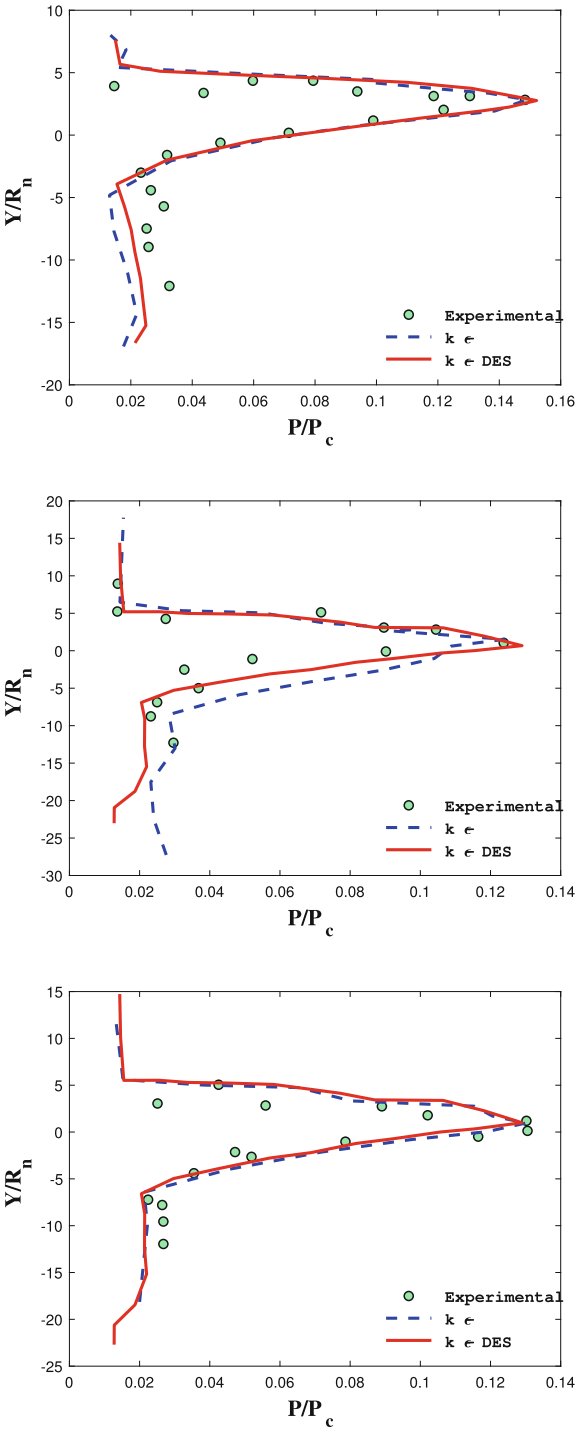

Fig. 3. Surface pressure distribution for $P_j/P_\infty = 7$ and $L/D_j = 2$, with different plate angles that are: (top) $\theta = 30°$, (middle) $\theta = 40°$, and (bottom) $\theta = 50°$, compared to experimental data [8].

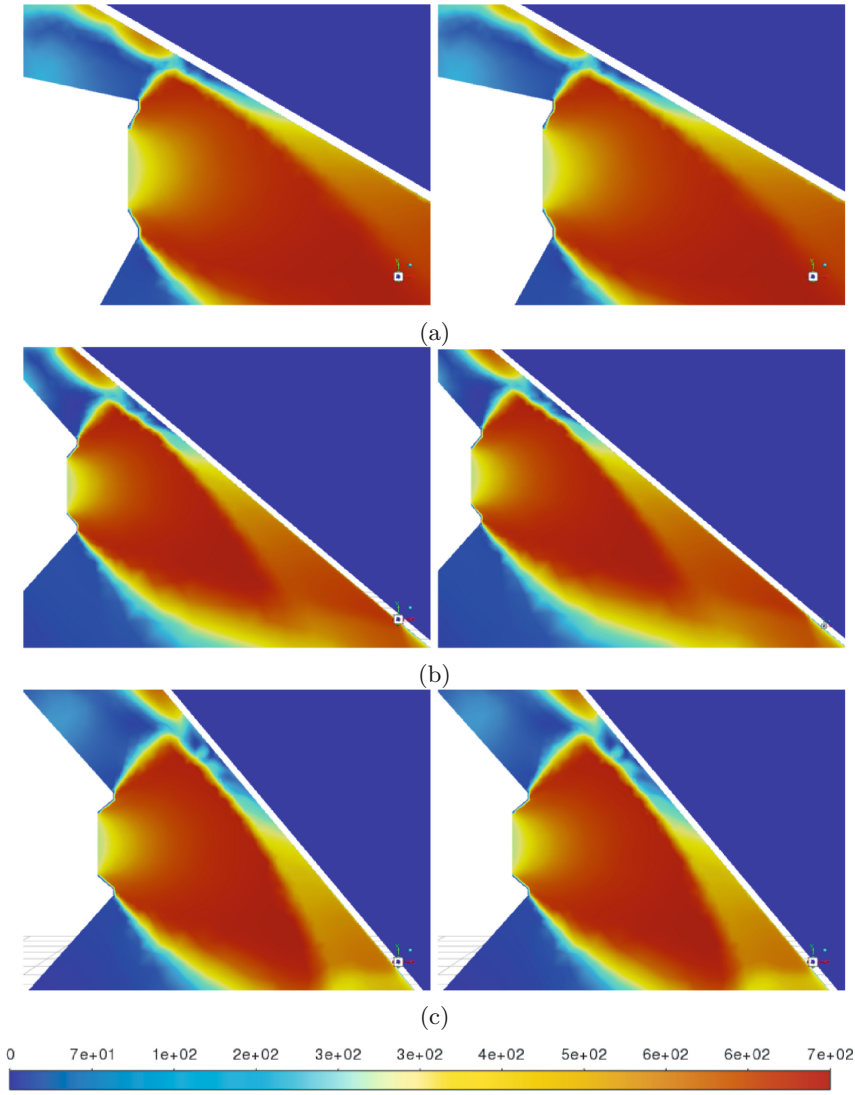

Fig. 4. Velocity contour map for URANS (left) and DES (right) calculations for $P_j/P_\infty = 7$ and $L/D_j = 2$ with different plate angles (a) $\theta = 30°$, (b) $\theta = 40°$, (c) $\theta = 50°$.

Figure 4 shows the velocity distribution in the symmetry plane corresponding to the flow region between the nozzle exit and the inclined plate. The complex structure of the three-dimensional mean flow field is apparent. The different characteristic features of the jet impingement, such as the jet boundary, jet shock, upper tail shock, front and behind plate shocks, are roughly captured. It is worth noticing how the expansion waves generated from the nozzle exit get reflected

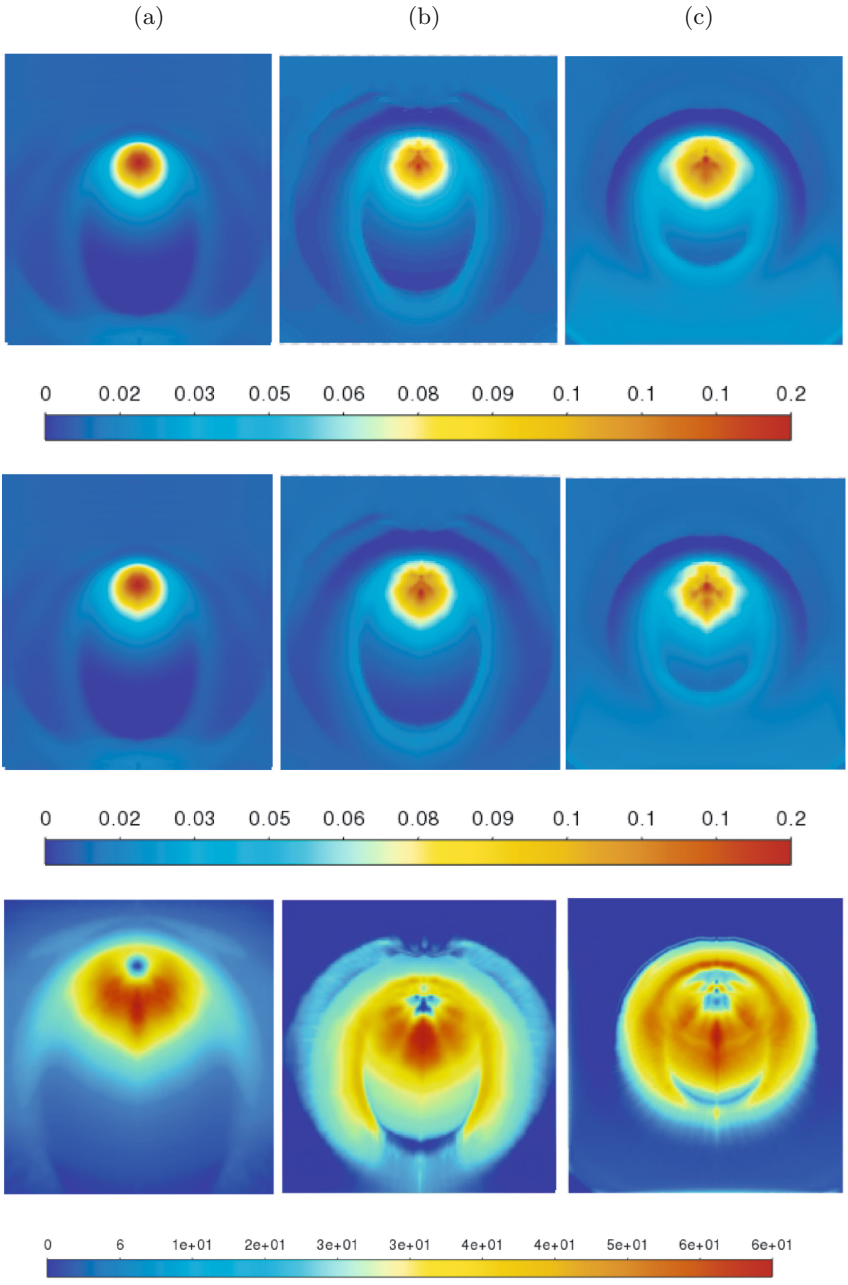

Fig. 5. Pressure (top), density (middle) and wall shear stress (bottom) contour maps for DES calculation at $P_j/P_\infty = 7$ and $L/D_j = 2$ with different plate angles (a) $\theta = 30°$, (b) $\theta = 40°$, (c) $\theta = 50°$.

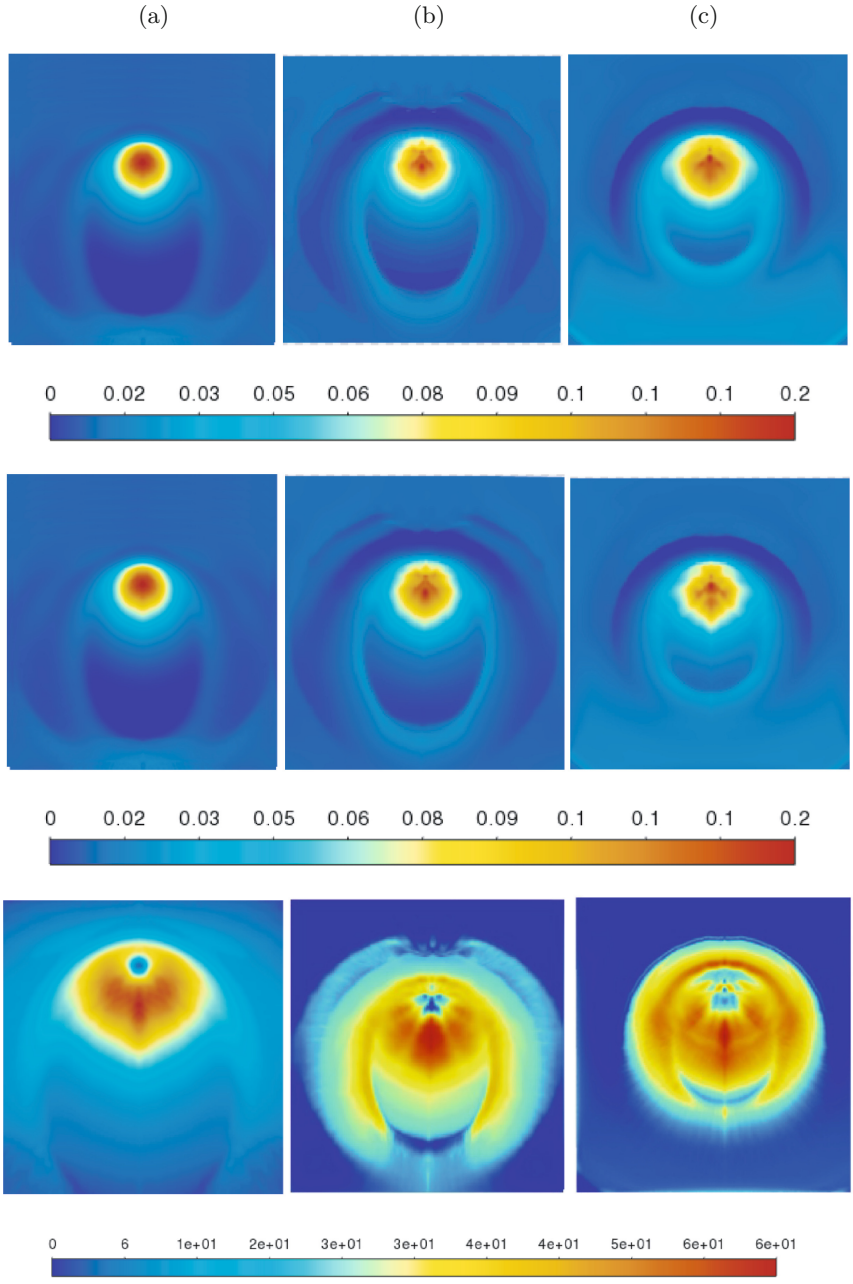

Fig. 6. Pressure (top), density (middle) and wall shear stress (bottom) contour maps for URANS calculation at $P_j/P_\infty = 7$ and $L/D_j = 2$ with different plate angles (a) $\theta = 30°$, (b) $\theta = 40°$, (c) $\theta = 50°$.

from the jet boundary and transform into compression waves which coalesce to form barrel shape jet shock. The Mach disc is formed very close to the plate. The contour maps of pressure, density and wall shear stress over the plate surface are presented in Fig. 5 and Fig. 6, for the URANS and DES solutions, respectively. These contour maps capture the features of the flow fields, for instance, the jet boundary. Again, the two different turbulence modeling procedures provide similar results.

4 Conclusions and Perspectives

Numerical simulations are carried out to simulate the supersonic jet impingement on an inclined flat plate at different angles of incidence, using two turbulence modeling approaches for predicting the mean flow field. Although more complicated turbulence models are widely used for this particular fluids engineering application, due to their completeness, this research shows that even a simpler (and faster) semi-empirical turbulence model such as the RNG $k-\epsilon$ model can be successfully adopted to the aim, resulting in saving computational resources.

Preliminarily, the overall CFD approach was validated using the RNG $k-\epsilon$ turbulence closure model supplied with wall functions, while reproducing the URANS data in the reference study, while making a comparison against experimental findings. Afterwards, a modern hybrid method, combining URANS and LES, namely, the DES approach was originally investigated. The results provided by the qualitative and quantitative analyses performed for the two different turbulence models demonstrate that both models correctly predict the pressure peak and its location on the plate, showing a good match with experimental results, regardless of the plate incidence.

As to future work, the next step of this ongoing research will be to extend our analysis to the thermal field, in particular by analysing the heat transfer coefficient, and the temperature distribution over the plate, in order to investigate the best pressure ratio ensuring the most efficient heat transmission. This will be done using innovative URANS approaches based on adaptive numerical methods [17,18], as well as improved DES formulations like the delayed detached-eddy simulation (DDES) [19], that will be examined in terms of computational effort and accuracy respect to the present methodologies.

Note that jet impingement cooling has demonstrated to achieve a high heat transfer coefficient compared to other traditional systems, resulting in higher heat transfer rates, which is essential, for instance, for modern hybrid vehicles. Since the main power source for such vehicles is provided by batteries, several studies have shown how these devices reach optimal operating conditions only when working in a particular temperature range, which is between 25 °C and 40 °C [20]. As a result, being able to manage their thermal performance is becoming crucial to their performance and safety. Jet air cooling systems also show several promising priorities when compared to other traditional methods such as: low cost, light weight and high reliability. Therefore, our future work for this particular fluids engineering application will also contribute to the development of jet cooling systems for hybrid and electric vehicles.

Acknowledgement. The authors acknowledge funding from the Italian Ministry of University and Research: PRIN research project 2022B2X937, "NextGenSProDesT Next Generation Space Propulsion Design Techniques."

References

1. De Stefano, G., Brown-Dymkoski, E., Vasilyev, O.V.: Wavelet-based adaptive large-eddy simulation of supersonic channel flow. J. Fluid Mech. **901**, A13 (2020)
2. Lubert, C.P., Kent, L.G., Seiji, T.: Supersonic jet noise from launch vehicles: 50 years since NASA SP-8072. J. Acoust. Soc. Am. **151**, 752–791 (2022)
3. Pamadi, B.N.: On the impingement of supersonic jet on a normal flat surface. Aeronaut. Quart. **13**, 199–218 (1982)
4. Chin, C., et al.: Investigation of the flow structures in supersonic free and impinging jet flows. J. Fluids Eng. **135**, 031202 (2013)
5. Nguyen, T., Maher, B., Hassan, Y.: Flow field characteristics of a supersonic jet impinging on an inclined surface. AIAA J. **58**, 1240–1254 (2020)
6. Lamont, P.J., Hunt, B.L.: The impingement of underexpanded, axisymmetric jets on perpendicular and inclined flat plates. J. Fluid Mech. **100**, 471–511 (1980)
7. Hadžiabdić, M., Hanjalić, K.: Vortical structures and heat transfer in a round impinging jet. J. Fluid Mech. **596**, 221–260 (2008)
8. Nakai, Y., Fujimatsu, N., Fujii, K.: Experimental study of underexpanded supersonic jet impingement on an inclined flat plate. AIAA J. **44**, 2691–2699 (2006)
9. Ito, M., Oyama, A., Fujii, K., Hayashi, K.: Flow field analysis of jet impinging on an inclined flat plate at high plate angles. In: Proceedings of the 44th AIAA Aerospace Sciences Meeting and Exhibit, Reno, Nevada, 9-12 January 2006 (2006)
10. Mixson J.S, Roussos L.A: Acoustic fatigue: overview of activities at NASA Langley. NASA Technical Memorandum 89143 (1987)
11. Wyatt L. A.: Static tests of ground effect on planforms fitted with a centrally-located round lifting jet. ARC/C **749** (1964)
12. Dharavath, M., Chakraborty, D.: Numerical simulation of supersonic jet impingement on inclined plate. Def. Sci. J. **4**, 355–362 (2013)
13. De Stefano, G., Denaro. F.M., Riccardi, G.: High-order filtering for control volume flow simulation. Int. J. Numer. Meth. Fluids **37**, 797–835 (2001)
14. https://www.ansys.com/products/fluids/ansys-fluent
15. Yakhot, V., Orszag, S.A., Thangam, S., Gatski, T.B., Speziale, C.G.: Development of turbulence models for shear flows by a double expansion technique. Phys. Fluids A **4**, 1510–1520 (1992)
16. Shih, T.-H., Liou, W.W., Shabbir, A., Yang, Z., Zhu, J.: A new $k-\epsilon$ eddy viscosity model for high Reynolds number turbulent flows. Comput. Fluids **25**, 227–238 (1995)
17. Ge, X., Vasilyev, O.V., De Stefano, G., Hussaini, M.Y.: Wavelet-based adaptive unsteady Reynolds-averaged Navier-Stokes computations of wall-bounded internal and external compressible turbulent flows. In: Proceedings of the 2018 AIAA Aerospace Sciences Meeting, Kissimmee, Florida, 8-12 January 2018 (2018)
18. Ge, X., Vasilyev, O.V., De Stefano, G., Hussaini, M.Y.: Wavelet-based adaptive unsteady Reynolds-averaged Navier-Stokes simulations of wall-bounded compressible turbulent flows. AIAA J. **58**, 1529–1549 (2020)
19. Salomone, T., Piomelli, U., De Stefano, G.: Wall-modeled and hybrid large-eddy simulations of the flow over roughness strips. Fluids **8**, 10 (2023)
20. Suh, I.S., Cho, H., Lee, M.: Feasibility study on thermoelectric device to energy storage system of an electric vehicle. Energy **76**, 436–444 (2014)